

HAPTIC RENDERING/CONTROL FOR UNDERACTUATED QB SOFTHAND USING HAPTION H GLOVE

N. (Nimish) Nadgere

MSC ASSIGNMENT

Committee:

dr. ir. J.F. Broenink
dr. ir. D. Dresscher
dr. ir. A.Q.L. Keemink

November, 2020

050RaM2020
Robotics and Mechatronics
EEMCS
University of Twente
P.O. Box 217
7500 AE Enschede
The Netherlands



Haptic rendering/control for underactuated QB SoftHand using Haption H Glove

Nimish B. Nadgere

Douwe Dresscher

Arvid Q.L. Keemink

Jan F. Broenink

Abstract—Haptic feedback plays a major role in improving performance and providing immersive experience in tele-manipulation tasks. Rendering haptic feedback in a system having large actuation and sensing asymmetries is a non-trivial problem. In this work, the synergy-based approach for control of the soft, adaptive robotic hand called QB SoftHand using a haptic exoskeleton called Haption HGlove is implemented. Shortcomings in the control method for applying kinesthetic force feedback in this synergy-based tele-manipulation system are identified and an alternative novel control method for generating force feedback is proposed. The feedback forces applied on the fingertips of the operator are experimentally evaluated by observing their magnitudes and directions. The effectiveness of the proposed tele-manipulation setup was verified using a relevant benchmarking test. The capability of the setup to distinguish between stiff and compliant objects could not be tested due to shortcomings in the implementation for estimating interaction forces. A study focused on improving the interaction force estimation capability of the system can better evaluate the proposed tele-manipulation in the future.

I. INTRODUCTION

A. Telerobotics

Telepresence, which is the virtual relocation of a human's senses, actions and presence to a distant location in real time, has the potential to solve numerous challenges faced by humankind. Telerobotics has a growing need in today's world where it can be crucial to provide a safe working environment to workforce employed in high-risk environments like the medical, disaster management or even nuclear sector. In unstructured environments, where pre-programmed task-planning for robots is difficult, telerobotic systems have a great advantage in executing versatile tasks which pertain not only to operation of machines and devices from a distance but also interaction with objects and their manipulation. They ensure safety of the human operator and also extend the capabilities of the human using scaling and filtering of the control signals. Incorporation of haptic feedback (force feedback) in the telemanipulation setup enhances task performance [23] in teleoperation activities. The problem of implementing a unified bilateral control framework for the control of a robotic hand, the QB SoftHand, intuitively using an exoskeleton, HGlove by Haption, for telemanipulation of objects is tackled in this work using a synergy-based mapping.

The goal of this study is aligned with the objective of the ANA AVATAR XPRIZE competition, that is, to create an immersive experience for the user to develop a sense of embodiment for controlling a distant robot in order to accomplish dexterous manipulation tasks in various scenarios.

The operator must be able to intuitively control the robotic hand only using fingertip positions sensed by the exoskeleton. The desired haptic feedback must act in a direction so as to oppose the operator's hand closure in order to simulate contact with an object in the remote environment.

Position tracking by the slave and effective haptic feedback for the master device are non-trivial problems in a bilateral system with large asymmetries in sensing and actuation.

B. QB SoftHand

The traditional robotic hand designs as discussed in [16] depend heavily on the ability to control force distributions at the contact points of the fingers and the object. Such force closure grasps, also referred to as stable grasps allow for successfully grasping a variety of objects irrespective of whether they are known to the user beforehand. In the race towards developing a highly dexterous robotic hand similar to the complex human hand, most of the robotic hands were developed with an approach towards boosting the complexity by means of a large number of DoFs and multiple sensors like the Utah/MIT hand [12], the Shadow hand [13], and the DLR-hand [7]. This approach compromises on the robustness and power capabilities due to delicate transmission of remote actuators and also control complexity due to the various actuators involved for grasping diverse objects. On the other hand, the practical approach followed by designers for grippers in industrial applications ensure ruggedness and simplicity largely to grasp only a few specific objects like in [15] and [21].

A novel approach that attempts to combine the desirable features of both the above approaches is inspired by the neuroscience behind how humans control the many DoFs of the human hand. Neuroscientific studies [20] indicate the existence of a high level control mechanism employed by the Central Nervous System to coordinate the movements of the several muscles of the human hand using reduced-dimensional synchronization patterns called eigen-grasps or hand synergies. The first two hand synergies account for around 80% of the variance of the hand grasp posture making the synergy space a very credible candidate for a basis for simplification of the grasping activities. In these studies, Principal Component Analysis (PCA) was applied to the joint angle data of human hands during grasping and the first two principal components referred to as PC1 and PC2 represented the hand pose for grasping a large variety of objects, with the higher principal components accounting for finer poses for specific objects.

These studies paved the way for novel strategies in not only control of fully actuated robotic hands but also their design. Dimensional reduction can be effectively applied to fully actuated robotic hands and their control algorithms as suggested in [9]. Mechanical implementations designed in [4] embedded these hand synergies into the hardware in order to reduce the number of actuators of the robotic hand and the control complexity.

The Pisa/IIT SoftHand [8] presents itself as a prime example of the product of the work on adaptive and soft synergies since it transfers the computational burden of synergies onto the mechanical design itself. The SoftHand is actuated using a single motor and uses only the motor position and motor current sensors for feedback, resulting in a highly under-actuated system. It performs hand closure only along the first synergy during unconstrained motion and under contact, its compliant property allows it to perform various poses upon interaction with any particular object. The full capabilities of the SoftHand for grasping various objects irrespective of whether they are known to the user in advance are explained in [3] where extensive experiments for its application in a robotic grasping competition were carried out. The effectiveness of the SoftHand for prosthetic applications highlights its intuitiveness and simplicity as shown in [11], [18] and [2].

In order to control a highly under-actuated system like the SoftHand in which its 19 DoFs are actuated and sensed only in the 1 dimensional space of the first synergy, a novel synergy-based control approach is required for intuitive telemanipulation.

C. Telemanipulation control of the QB SoftHand

A study of the efficacy of haptic feedback in prosthetic application involving teleimpedance control using the SoftHand [1] first proposed the technique for estimating the environmental forces acting on the SoftHand without making use of additional sensors. It describes an interaction torque observer that can effectively compensate the frictional, inertial and stiffness related torque contribution of the SoftHand's motor to provide interaction torque that can be used to calculate haptic feedback. The idea of a unified control framework for bilateral telemanipulation which acts as an intermediate control layer abstracting the specific kinematics of the hardware was first suggested in [10]. Such a traditional mapping of the operator's motions cannot be applied to the SoftHand due to the absence of specific joint information and actuation capability for its various joints.

Since the core design of the SoftHand is rooted in neuroscience, the appropriate control framework for its bilateral telemanipulation can also be derived from the concept of synergies as is presented in [5]. In this paper, the concept of synergies obtained from dimensional reduction of joint position data is applied and verified for synergies obtained from fingertip data in Cartesian space leading to the generation of a Cartesian based Synergy Matrix which acts as a mapping between fingertip data in Cartesian Space and Synergy Space. The feedback forces to be applied on the fingertips

of the operator are obtained by applying the same power-continuous synergy mapping on forces in synergy space. The same interaction torque mentioned earlier in [1] is assigned as the sole non-zero feedback force reference in synergy space. Experimental results in [5] and [6] of this synergy-based bilateral port applied to a telemanipulation setup involving the SoftHand along with HEXOTRAC, a 3 fingered haptic device with only 1 active joint per finger suggest effective grasping for various objects.

D. HGlove

The master device used for telemanipulation in this study is the HGlove by Haption [17] which is a 3 fingered exoskeleton device having a serial manipulator each for the thumb, index finger and the middle finger. Each finger has 3 articulations, the first for the ulnar deviation, that is adduction and abduction, and the other two for the phalanges. The design of the HGlove allows users of any hand size to wear it and their fingertip positions in Cartesian space can be effectively obtained. The angular position of all three joints can be sensed, but feedback torque can only be applied to the second and third joints via their DC motors. Therefore the two active joints per finger ensure that complete haptic feedback can be provided to the fingertips in their plane of flexure, even if none can be provided in the direction of adduction or abduction.

E. Problem Statement

As mentioned in section I-C, the work presented in [5] is the first to apply synergy based control in telemanipulation. However, there is a fundamental shortcoming in the force feedback generation proposed in the existing work with regards to the direction of the reference feedback forces. These forces act, as proved later in section II-B1, in fixed and time-invariant directions which depend on the synergy mapping generated. The experiments undertaken to evaluate the flawed force feedback generation likely overlooked the shortcomings due to two reasons, namely the highly underactuated master device and the lack of variety in size of the objects grasped to evaluate the force feedback.

Additionally, since the SoftHand follows position commands solely along PC1, there is a possibility of significant mismatch between the operator's intended pose moments prior to grasping an object and the PC1 position command that the operator's deviated pose would send to the SoftHand to follow. An example of such a scenario could be if the user decides to stick a particular finger out habitually to grasp an unusual object. This mismatch could potentially be a big source of interruption of the haptic experience for the user.

F. Goal

In order to overcome the shortcomings of the existing implementation stated in I-E, an alternative method to generate force feedback references is proposed. It is also evaluated to ensure that the direction of force feedback applied on the operator's fingertips effectively simulates contact with objects for the tasks of grasping objects. Since the robotic hand under

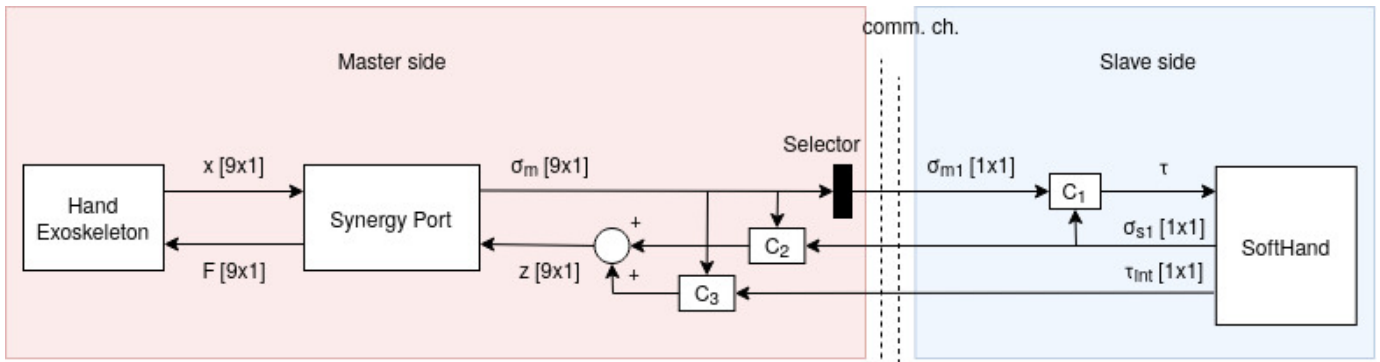


Fig. 1. Overview of proposed bilateral telemanipulation setup

consideration is soft and adaptive, interaction forces estimated from the SoftHand’s motor, explained further in section II-B3, are applied as reference feedback forces. In addition to these forces, it is proposed to apply impedance control, explained further in section II-B2, in order to guide the operator’s hand-pose to match that of the SoftHand at all times. An evaluation of the haptic feedback in grasping tasks for various objects of a range of shapes and sizes is carried out to determine the effectiveness of the implemented telemanipulation setup for grasping activities.

The mapping from cartesian to synergy space, necessary to understand the shortcomings of the existing implementation, is described in the next section based on the particular methods applied for the hardware under consideration.

II. METHODS

This section describes the methods implemented to realise the idea proposed in the previous section. Firstly, section II-A describes the synergy-based mapping in detail along with its implementation for mapping position data using the hardware under consideration. Next, section II-B deals with mapping force data from synergy space to cartesian space. It states the shortcomings of the existing implementation in doing so and presents the alternative control methods implemented in this work to overcome them.

A. Synergy-based Mapping

This section is dedicated to extraction of reduced dimensional data from the operator’s fingertip trajectory in order to be used as position setpoint for the slave device.

1) *Concept of Synergy Mapping:* Research by Santello and colleagues [20] first used the Principal Component Analysis (PCA) to find that the joint displacement data of human hands exhibit high correlation amongst the joints and that the identified independent directions can describe the posture of human hands in a reduced dimensional space called the hand synergies. The hand pose can therefore be described in the reduced dimensional synergy space by neglecting higher principal components without significant loss in quality of data. There is extensive research that has built upon this ability

of feature extraction from higher dimensional data applied to joint space of the hand.

A. Brygo and colleagues [6] applied an analogous PCA based analysis to fingertip motion in cartesian space and established the feasibility of creating a similar cartesian-based synergy space. In this work, this same PCA based analysis is applied to generate a mapping which facilitates a change of base of fingertip coordinates between synergy space and cartesian space using the HGlove as the exoskeleton. For PCA, the data collection experiment requires the dimension of the space used to describe the position of each fingertip to be 3 which is possible with the HGlove. The synergy mapping was created in the form of a synergy matrix S_x whose column vectors are the eigenvectors of the covariance matrix of the mean-centered data. Cartesian-based synergies will hereafter be referred to simply as synergies unless stated otherwise.

2) *Extraction of First Synergy Position Coordinate:* The exoskeleton provides position information in the form of displacements q in the joint space of its 3 fingers using position encoders. The displacements in joint space are required to be transformed to cartesian space using Forward Kinematics of the exoskeleton finger as shown in equation 1, which is in this case, a 3 DoF serial manipulator since the joint displacements $q(t) \in \mathbb{R}^m$, where $m = 3$ represents the number of joints of each exoskeleton finger.

$$x(t) = f_k q(t) \quad (1)$$

Next, the fingertip cartesian position data $x(t)$ is centered around the mean obtained from PCA analysis and the resulting vector $X(t)$ contains the mean-centered fingertip position in cartesian space stacked in a single vector $X(t) \in \mathbb{R}^9$.

Finally, the synergy mapping is used to perform a change of base of the mean-centered fingertip position data from cartesian space to synergy space using equation 2

$$\sigma(t) = S_x^{-1} X(t) \quad (2)$$

where $\sigma(t) \in \mathbb{R}^{mn}$ and $S_x \in \mathbb{R}^{mn \times mn}$ with $mn = 9$ in this case. The first element of the position in synergy space σ_1 is extracted and scaled to the SoftHand’s motor range. The SoftHand uses σ_1 as the position reference to be tracked by its PI motor controller using current commands. The system is

experimentally tested to ensure it follows the outcomes stated in the experimental validation of the position mapping into synergy space laid out in [6].

One of the two validation experiments involves motion of the operator’s hand along first synergy, i.e. hand closure to grasp a random object leading to corresponding change in the position along first synergy, σ_1 as can be seen in figure 2. It is noteworthy to observe that the coordinates along higher synergies σ_2 to σ_9 also vary during hand closure although in small amounts. The synergy space trajectory in Figure 2 provides insight about the position mapping process of the hand pose in synergy space. It extracts data from a higher dimensional space to a lower dimensional space with a small loss of information. This is evident by the observation that if a hand closure deviating from the one along PC1 is made by the operator, the QB SoftHand fails to track it exactly and it instead follows only the PC1 coordinate of the hand-pose.

The following section describes the equivalent synergy mapping to generate cartesian force feedback references for the exoskeleton from the synergistic forces.

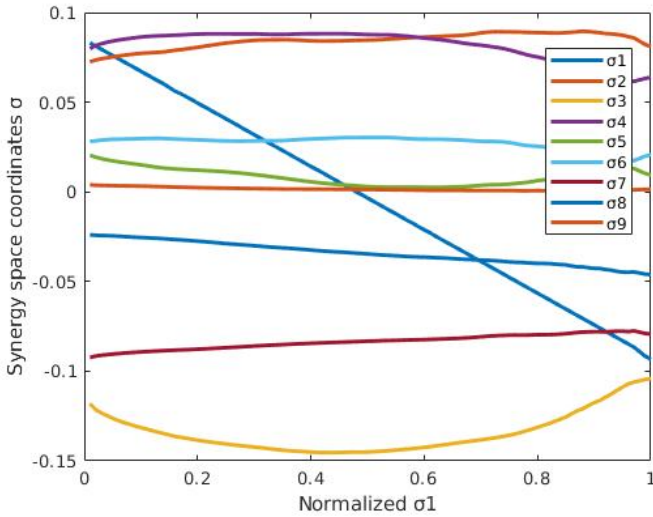


Fig. 2. Synergy Space trajectory σ of operator’s hand during PC1 motion calculated using fingertip positions

3) *Mapping synergy-based forces to cartesian space:* The synergy mapping stated earlier in section II-A1 is a power continuous transforming action performing a change of base between synergy space and cartesian space, since it can be applied using the synergy matrix S_x which is a linear, time-constant operator. Equation 3 was derived in [6] by applying the power balance equation between the cartesian and synergy bases using the synergy matrix.

$$F(t) = S_x^{-T} z(t) \quad (3)$$

where $F(t) \in \mathbb{R}^{mn}$ represents the fingertip force vectors in cartesian space stacked in a single vector calculated as a projection of the feedback forces $z(t) \in \mathbb{R}^{mn}$ in synergy space.

After the cartesian force reference $F(t)$ is obtained, it is then mapped to the exoskeleton’s joint space using

$$\tau_{exo}(t) = J(q)^T F(t) \quad (4)$$

where $\tau_{exo} \in \mathbb{R}^{mn}$ represents the exoskeleton torque vector containing a stack of joint torques to be applied to each of the fingers of the exoskeleton and $J(q) \in \mathbb{R}^{3m \times 3n}$ is the exoskeleton Jacobian from which the columns corresponding to cartesian torques are eliminated.

The next section discusses control methods to generate reference feedback forces $z(t)$ in synergy space.

B. Synergy-Based Force Feedback

The method of incorporating interaction forces in the existing force feedback implementation proposed in [6] leads to some fundamental shortcomings explained in detail in section II-B1. In an ideal scenario, the fingertip force feedback exactly reflects the forces acting on the slave hand’s fingertips. An alternative control method for generating feedback force references is proposed to reflect the interaction forces from the slave device in section II-B3. This is supplemented with a hand-pose tracking control method in section II-B2 to ensure that the hand-pose of the slave device is closely followed. Figure 3 is a detailed control diagram of the proposed bilateral telemanipulation setup.

1) *Shortcomings of existing implementation:* The force feedback strategy undertaken in [6] and [5] assigns the interaction torque estimated from the SoftHand’s motor as the first element of an empty force vector $z(t)$ as represented in equation 5.

$$z(t) = [\tau_{int} \ 0 \ \dots \ 0] \quad (5)$$

This synergy space reference feedback force mapped to cartesian space using equation 3 leads to a cartesian force vector having a fixed direction and scaled by the interaction torque τ_{int} because the synergy matrix S_x is time-constant. The cartesian force feedback vector in the existing implementation is stated in the following equation,

$$F(t)_{[9 \times 1]} = (S_x^{-T})_{[9 \times 1]} \tau_{int}$$

These forces may act in the desired direction for a particular closure of the hand, that is, for a particular size of an object, but not for objects of different sizes. The experimental results for the existing implementation show feedback forces having directions which do not appear to clearly oppose hand closure and instead they guide the fingers to curl up inwards which is very unlike the reaction forces that the human hand faces roughly normal to the surface of the object grasped. This direction of the fingertip forces are fixed based on the synergy matrix and do not vary with the configuration or posture of the hand. Therefore, non-zero forces along higher principal components in synergy space, that is, $z_{2,3,\dots}$ are necessary to provide meaningful force feedback to the operator for objects of various sizes. An attempt is made to define the requirements for meaningful force feedback in section II-B3. A control method to ensure hand-pose tracking along PC1 is described in detail in the next section.

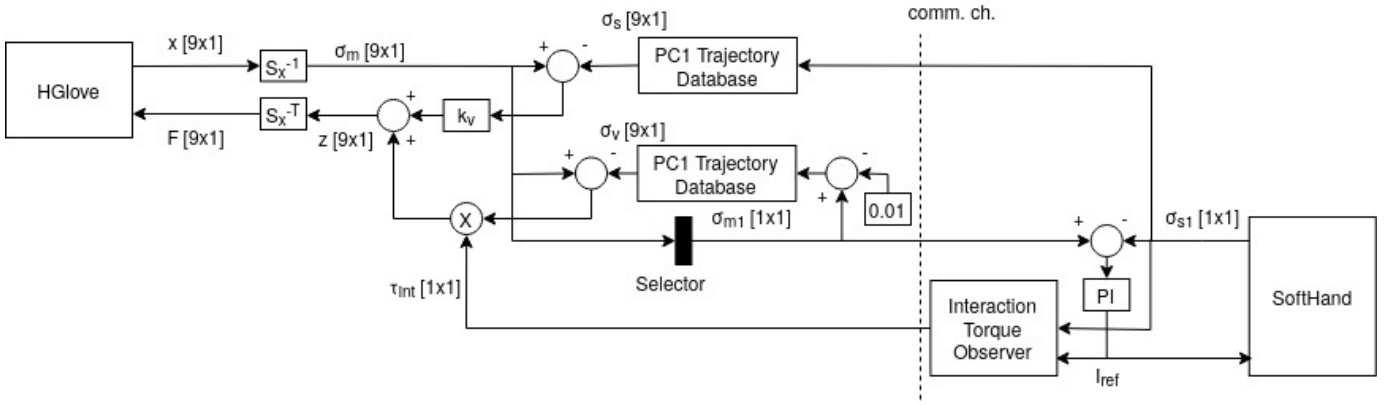


Fig. 3. Control diagram of the implemented telemanipulation setup

2) *Feedback forces for PC1 hand-pose tracking:* In order to ensure hand-pose tracking along PC1, impedance control is applied in synergy space to the position difference of the exoskeleton and the robotic hand resulting in generation of reference feedback forces in synergy space $z(t) \in \mathbb{R}^{3m}$. Since the SoftHand only provides position feedback from its motor which corresponds to the position coordinate along PC1, the coordinates along higher principal components need to be estimated.

These higher synergy position coordinates of the hand closure motion can be observed in the figure 2 where the operator performed hand closure in a manner identical to that of the SoftHand. These coordinates must be obtained from an operator-specific database because they may differ from person to person and they are complex functions of the hand closure σ_1 . This synergy space pose σ is recorded for 100 intervals between the range of SoftHand's closure σ_1 during a simplified calibration procedure. This simplified calibration, as stated in [5], is required to be performed for every new operator.

A database $\sigma_{database} \in \mathbb{R}^{3m \times 100}$ of this synergy space pose, therefore, contains the setpoints σ of the operator's hand trajectory along the first synergy identical to the SoftHand's motion. During operation, this setpoint database is accessed with an index corresponding to the position σ_{s1} of the slave device to estimate the virtual position of the slave device along higher principal components. A constant virtual stiffness k_v is attached between this virtual slave position σ_s as the setpoint and master position σ_m to generate reference feedback forces $z_{pos}(t)$ in synergy space.

This control method is based on the assumption that an impedance controller in synergy space will act similar to one in cartesian space and will generate synergy space forces corresponding to the position difference in synergy space. These synergy space forces may be non-zero for higher synergies unlike in previous work, as pointed out in section II-B1. The synergy space forces calculated in this way, after being mapped to cartesian space, can guide the fingertips intuitively to the PC1 hand-pose recorded for the operator beforehand.

In case the operator's hand-pose is already along PC1, the feedback forces generated will be roughly zero or insignificant, and once any of the fingers deviate from the PC1 trajectory recorded in the database, the feedback forces will be generated in a direction which will guide the fingers back to a hand-pose along PC1. This way, depending on the value of the virtual stiffness of the impedance controller, the operator's fingers will not be able to deviate too far from a hand-pose along PC1 and they will track the hand-pose of the SoftHand correctly until it makes contact with an object.

Equation 6 represents this impedance controller applied to position difference in synergy space to generate reference force feedback $z_{pos}(t)$

$$\begin{aligned} z_{pos}(t) &= k_v (\sigma_s - \sigma_m) \\ \sigma_s &= \sigma_{database} [\sigma_{s1}] \end{aligned} \quad (6)$$

An important feature of this controller for hand-pose tracking is that it guides the operator using finger-specific force feedback to match the hand pose of the SoftHand during unconstrained motion in the event that the operator deviates from motion along the first synergy by way of habit for certain objects. The full extent of the haptic capabilities of the haptic device are utilised to minimize this mismatch by guiding the user's fingers along the first synergy using haptic feedback.

In the absence of this haptic guiding feature of the hand-pose tracking controller, the workload of minimizing this mismatch would solely depend on visual feedback of the user, which is not efficient from the perspective of task performance. More so, after contact with an object, the force feedback due to interaction forces on a finger that may deviate from the PC1 hand-pose would be unintuitive and in the incorrect direction. Therefore, this haptic guiding feature could be highly beneficial in achieving immersive haptic experience for the operator.

As soon as the SoftHand makes contact with the environment, there is uncertainty about the SoftHand itself following the first synergy and the ensuing mismatch is unavoidable. Therefore, after contact is made, the force feedback provided to the operator will continue to be generated along the first

synergy and it will be identical to the case of squeezing a spherical ball regardless of the shape of the actual object being grasped.

In case this control method alone is implemented, the force feedback would solely be due to the SoftHand’s motor position, which has previously been used only for proprioceptive feedback [18], [2]. Haptic feedback arising from interaction forces acting on the soft and adaptive SoftHand requires additional effort-related data from the SoftHand. The next section deals with the control method that generates force feedback references due to interaction forces estimated from the state information of the SoftHand’s motor.

3) *Feedback forces due to remote interaction:* As discussed earlier in section II-A3, the interaction torque τ_{int} estimated from the SoftHand’s motor is a scalar or a low dimensional quantity that can only provide information about the magnitude of the interaction forces and not their directions. For immersive force feedback, the forces provided as feedback to the operator must reflect the forces experienced by the robot in the remote environment. The forces on the fingertips of the SoftHand upon contact with any object arise as reaction forces acting normal to the surface of the object. These reaction forces oppose hand closure and therefore have a direction opposite to that of the hand closure. The objective of force feedback due to interaction forces is to simulate contact with an object in the remote environment which naturally leads to two requirements expected of the reference feedback forces:

- 1) The directions of the feedback forces must be opposite to the direction of hand closure
- 2) The magnitude of the feedback forces must reflect the magnitude of the interaction forces acting on the slave hand

The interaction forces are proposed to be calculated by directing the estimated interaction torque along a vector in synergy space directed towards a more open hand-pose than the master’s current hand pose. The first requirement is satisfied by determining the direction-vector as a unit vector between the current hand pose of the operator and a virtual setpoint hand-pose that opposes hand closure. The second requirement is satisfied by using the estimated interaction force as the magnitude.

$$z_{int}(t) = \tau_{int} \frac{(\sigma_v - \sigma_m)}{|\sigma_v - \sigma_m|} \quad (7)$$

$$\sigma_v = \sigma_{database} [\sigma_{m1} - c]$$

Equation 7 shows the equations used to generate force feedback reference $z_{int}(t)$ due to remote interaction where c and τ_{int} are tuned so that the maximum force is limited to that of the exoskeleton’s specifications. The virtual setpoint hand-pose here is obtained by accessing the setpoint database, described in the previous section II-B2, with an index corresponding to $\sigma_{m1} - c$ which is a hand pose more open than the current hand pose σ_{m1} . Here $\sigma_{m1} \in [0, 1]$ is the normalized PC1 coordinate of the master and $0 > c > 0.01$ is an offset chosen as a fixed position difference to calculate the directions of forces.

$$z(t) = z_{int}(t) + z_{pos}(t) \quad (8)$$

Following the four-channel architecture described in [14], the hand-pose tracking control component $z_{pos}(t)$ based on slave position reference and the slave dynamic component $z_{int}(t)$ based on the interaction forces exerted by the environment are summed and applied as reference force feedback $z(t)$ to the master device as stated in equation 8.

The experimental setup and considerations made to evaluate the telemanipulation setup that is implemented in this work are described in the next section.

III. EXPERIMENTS

In this section, experiments are carried out to assess the proposed bilateral telemanipulation setup in terms of quality of force feedback and effectiveness in grasping activities. The experimental setup consists of the SoftHand controlled by the HGlove via the synergy port framework which generates force feedback using a combination of the impedance method and the interaction method.

A. Force Feedback Characterization

The force feedback applied at the fingertips is characterized by the magnitude of the force acting on each fingertip and the direction of the force with respect to the fingertip.

1) *Magnitude of force feedback:* The magnitude of the force feedback is examined in an experiment where the operator performed the same grasping motion under 3 different conditions. The first trial is performed in free space, in the second trial a soft object is grasped and in the third trial a stiff object is grasped. The soft object taken here is the cylindrical part of a neck pillow roughly 8cm in diameter and the stiff object is a cylindrical plastic bottle of the same size as shown in figure 4. The magnitude of the forces on every finger are compared with the commanded slave position σ_1 , motor torque τ_m and interaction torque τ_{int} to demonstrate the abilities of the system to reflect the various impedances of the environment.

2) *Directions of force feedback:* Two sets of experiments are carried out in order to evaluate the force feedback caused by two separate events-

- hand closure leading to contact with object
- deviation of operator’s hand pose from closure along first synergy

In both sets of experiments, the directions of the forces applied are observed using the reference feedback forces plotted on the $X - Y$ plane of each finger for a clear view over the course of their trajectory. The object chosen is a stiff spherical ball of diameter 8cm to simulate contact at hand closure roughly equal to 70%. In this case, the directions of the forces are compared against the desired directions of forces which are always opposing the closure of the hand at any position and are expected to be normal to the surface of the object. In the case of deviation from open hand pose, only one finger is made to deviate from the PC1 hand-pose at a time such that the direction of force on the deviated finger guides it back to a PC1 hand-pose.



Fig. 4. The stiff and compliant object grasped for observing the magnitude of forces

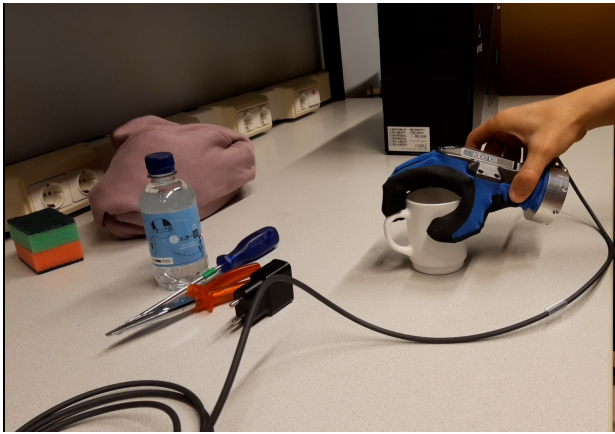


Fig. 5. The experimental setup for testing effectiveness of the system

B. Effectiveness in grasping activities

Based on the benchmarking test proposed in [22], a simplified experiment to evaluate the effectiveness of the bilateral telemanipulation setup involving the SoftHand and the HGlove is undertaken. In this experiment, an operator is performing the activity of reaching for the objects, grasping them securely and placing them in a different location. Since the focus is on the hand and not on the position of the wrist, the SoftHand was held by an assistant in the required position in order to grasp the objects and transport them. The 8 objects under consideration consist of 6 rigid objects: a water bottle, a pair of pliers, a phone charger, a screw driver, a spray bottle, a cup and 2 compliant objects: dish-washing sponge and a rolled-up tshirt. These objects were chosen to represent a wide variety of shapes and stiffnesses. Figure 5 shows the QB SoftHand and the objects.

A scoring system was followed similar to the proposed benchmarking test, but the approach elevation and hand orientation were not varied since the objective is to evaluate the telemanipulation setup and not to test the capabilities of the robotic hand. For each object, the activity was repeated 10

times and a score was assigned to each attempt based on the following conditions:

$$s_g = \begin{cases} 0 & \text{object not grasped} \\ 0.5 & \text{object lost in transit} \\ 1 & \text{grasp cycle completed} \end{cases} \quad (9)$$

The mean and standard deviations of these scores were representative of the effectiveness and robustness of the telemanipulation system in grasping the respective object.

IV. RESULTS & DISCUSSION

In this section, the results of the experiments are presented and discussed to make inferences about the proposed bilateral telemanipulation setup.

A. Force Feedback Characterization

1) *Magnitude of Force Feedback*: Figure 6 shows the magnitude of the force feedback F applied on fingertips of the individual fingers as a function of time as the hand closure was performed for 3 trials- no object, soft object and stiff object. The plots also contain the corresponding normalized PC1 coordinate of hand closure σ_1 , interaction torque τ_{int} estimated from the interaction torque observer and the current I_{ref} of the SoftHand's motor used to estimate the interaction torque.

The interaction torque is expected to reflect only when contact with the object is made, but the implementation of the interaction torque observer allows a small peak at the beginning of hand closure ($0 < \sigma_1 < 0.2$). This peak can be attributed to a position-dependent singularity due to friction deviating from the expected profile of torque due to friction modelled in the Interaction Torque Observer block of the control setup. This reasoning is verified by the peak observed in the current I_{ref} obtained from the SoftHand motor which is used to estimate the interaction torque.

In the first trial, as expected, the interaction torque is close to zero during the closure of the SoftHand because there is no interaction with any object. In the other two trials, interaction torque is high after contact with the object as expected until the hand begins to open. The difference between the second trial of the soft object and the third trial of the stiff object is that, after contact, the position of the SoftHand's motor keeps changing in the case of the soft object due to its compliance during the 'object squeezing' phase of the closure, whereas in the case of the stiff object, there is negligible change in the position since the stiff object cannot be squeezed. It appears that the interaction torque on contact varies marginally in magnitude compared with the soft and rigid objects indicating that the implementation of the interaction torque observer could not effectively make a distinction between compliant and stiff objects in this experiment.

The main objective of this experiment is to observe the magnitude of the finger-specific forces during the different stages of the hand closure. The finger-specific force feedback follows the interaction torque very effectively despite the small deviations which are attributed to the impedance control

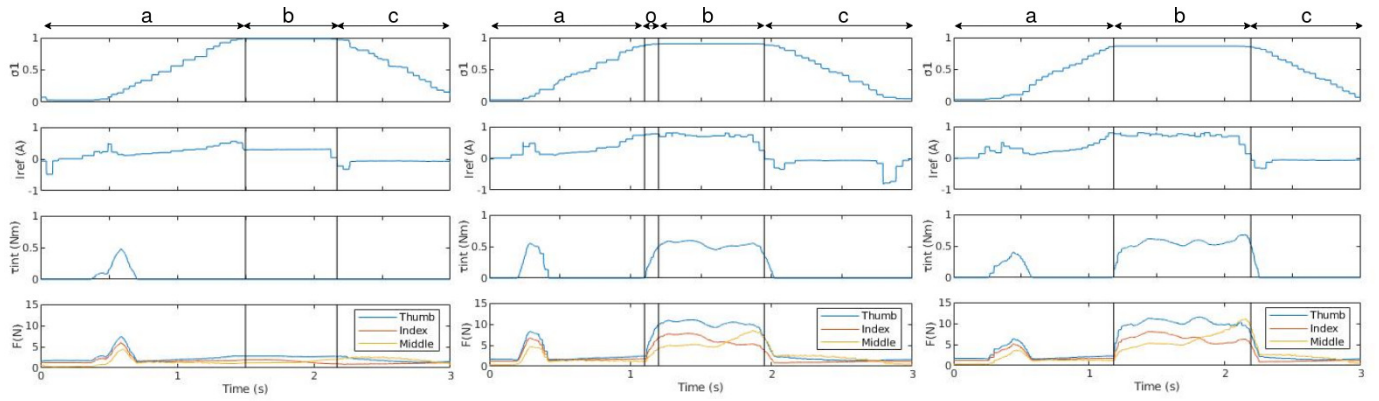


Fig. 6. Force Feedback magnitude during hand closure over 3 attempts: (left-right) no object, soft object, stiff object
a - closing phase, b - fully closed, c - opening phase, o - object squeezing phase

guiding the fingers that are deviating from a hand pose along first synergy. Therefore, the magnitude of the feedback forces indicate that the interaction forces acting on the QB SoftHand are satisfactorily reflected.

2) *Directions of Force Feedback*: The directions of the forces during hand closure is represented in figure 8 where a spatial map of the $X - Y$ plane of each finger is used to plot the fingertip forces marked with 'x' starting from fingertip positions marked with 'o'. Figures of a finger and an object are added to aid in visualizing the contact taking place and the directions that the forces are expected to act in. It can be seen that the forces coloured red, that is, during closed hand pose are larger and oppose hand closure at every instance. In comparison, the forces coloured green, that is, during open hand pose are significantly smaller and may exist due to the PC1 hand-pose tracking feature. The feedback forces during contact act roughly normal to the surface of the object as reaction forces are expected to do. Therefore, it can be said that requirements expected from directions of force feedback are satisfied since they oppose hand closure effectively.

The PC1 hand-pose tracking feature of the impedance-based controller is demonstrated in the second experiment where the operator moved each of their fingers, one at a time, deviating from the open hand-pose. The directions of forces for each deviated finger in figure 7 point back to the original position indicating that the feedback force guides the finger back to a hand-pose along first synergy. These forces were very small in the previous experiment where the operator's hand pose did not deviate from the PC1 hand-pose trajectory. The proposed hand-pose tracking feature of the controller, therefore, ensures that the operator's hand-pose matches that of the slave device.

B. Effectiveness in grasping activities

Applying the scoring system defined in section III, perfect scores (mean and standard deviation of 10 trials) were obtained for each trial by the operator. Since the operator could decide the approach elevation and hand orientation for the objects, favourable combinations of the two were adopted. All the

attempts were completely successful indicating that the proposed telemanipulation control setup is effective in grasping activities.

V. CONCLUSION

This paper presented a novel impedance-based control algorithm to generate effective kinesthetic feedback forces in a bilateral telemanipulation system having large asymmetries in terms of kinematics, sensing and actuation. The shortcomings in existing work were overcome using a variable impedance control method in a synergy-based telemanipulation framework. A haptic guiding feature which guides the operator's fingertips towards the slave robot's estimated hand pose was introduced to improve the immersive experience of the operator during the telemanipulation activities. The setup involved the QB SoftHand as the robotic hand controlled by the Haption HGlove as the hand exoskeleton. Experiments were carried out to prove the effectiveness of the proposed control algorithm in activities of grasping objects of a variety of shapes and sizes. The impedance of the objects could not be reflected effectively in the experiments due to shortcomings in the implementation for estimating interaction forces.

Future work to evaluate the proposed control algorithm with effective reflection of interaction forces could demonstrate the impedance reflection capabilities of the system. A further evaluation of the effectiveness of telemanipulation system of the hand mounted on an arm of a humanoid robot can be carried out in detail in reach-grasp-transport tasks.

REFERENCES

- [1] Arash Ajoudani et al. "Exploring teleimpedance and tactile feedback for intuitive control of the pisa/iit softhand". In: *IEEE transactions on haptics* 7.2 (2014), pp. 203–215.
- [2] Edoardo Battaglia et al. "The Rice Haptic Rocker: skin stretch haptic feedback with the Pisa/IIT SoftHand". In: *2017 IEEE World Haptics Conference (WHC)*. IEEE, 2017, pp. 7–12.

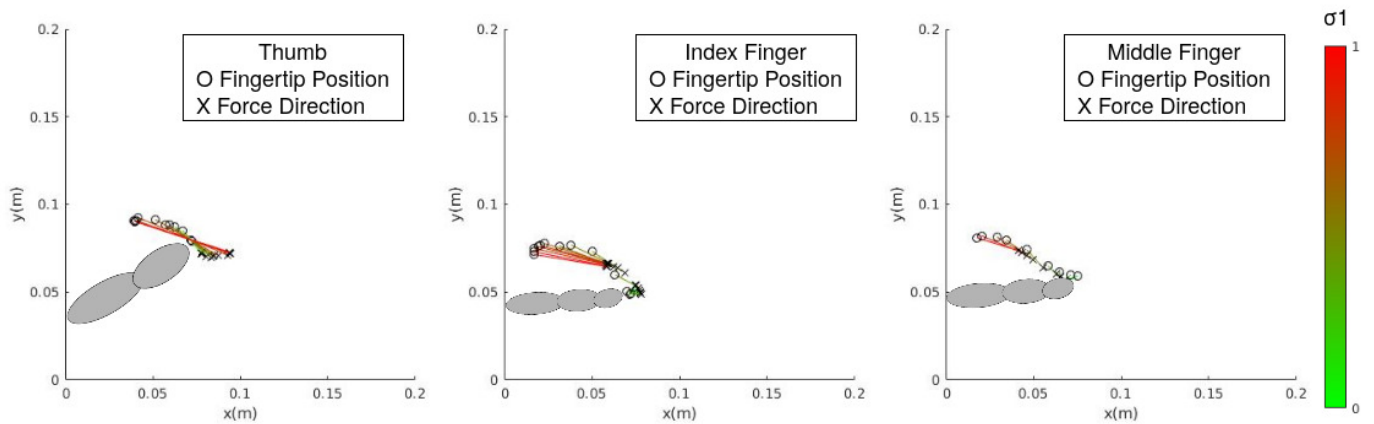


Fig. 7. Hand-pose tracking for individual fingers upon deviation from first synergical hand pose. Left-right: Thumb, Index, Middle

- [3] Manuel Bonilla et al. “Advanced Grasping with the Pisa/IIT SoftHand”. In: *Robotic Grasping and Manipulation Challenge*. Springer, 2016, pp. 19–38.
- [4] Christopher Y Brown and H Harry Asada. “Inter-finger coordination and postural synergies in robot hands via mechanical implementation of principal components analysis”. In: *2007 IEEE/RSJ International Conference on Intelligent Robots and Systems*. IEEE, 2007, pp. 2877–2882.
- [5] Anais Brygo et al. “Synergy-Based Bilateral Port: A Universal Control Module for Tele-Manipulation Frameworks Using Asymmetric Master-Slave Systems”. In: *Frontiers in bioengineering and biotechnology* 5 (2017), p. 19.
- [6] Anais Brygo et al. “Synergy-based interface for bilateral tele-manipulations of a master-slave system with large asymmetries”. In: *2016 IEEE International Conference on Robotics and Automation (ICRA)*. IEEE, 2016, pp. 4859–4865.
- [7] Jörg Butterfaß et al. “DLR-Hand II: Next generation of a dextrous robot hand”. In: *Proceedings 2001 ICRA. IEEE International Conference on Robotics and Automation (Cat. No. 01CH37164)*. Vol. 1. IEEE, 2001, pp. 109–114.
- [8] Manuel G Catalano et al. “From soft to adaptive synergies: The Pisa/IIT SoftHand”. In: *Human and Robot Hands*. Springer, 2016, pp. 101–125.
- [9] Matei Ciocarlie, Corey Goldfeder, and Peter Allen. “Dimensionality reduction for hand-independent dextrous robotic grasping”. In: *2007 IEEE/RSJ International Conference on Intelligent Robots and Systems*. IEEE, 2007, pp. 3270–3275.
- [10] Guido Gioioso et al. “Mapping synergies from human to robotic hands with dissimilar kinematics: an approach in the object domain”. In: *IEEE Transactions on Robotics* 29.4 (2013), pp. 825–837.
- [11] Sasha B Goffrey et al. “A synergy-driven approach to a myoelectric hand”. In: *2013 IEEE 13th International Conference on Rehabilitation Robotics (ICORR)*. IEEE, 2013, pp. 1–6.
- [12] Steve C Jacobsen et al. “The UTAH/MIT dextrous hand: Work in progress”. In: *The International Journal of Robotics Research* 3.4 (1984), pp. 21–50.
- [13] Anna Kochan. “Shadow delivers first hand”. In: *Industrial robot: an international journal* (2005).
- [14] Marco Laghi et al. “Unifying bilateral teleoperation and tele-impedance for enhanced user experience”. In: *The International Journal of Robotics Research* 39.4 (2020), pp. 514–539.
- [15] Serge Montambault and Clément M Gosselin. “Analysis of underactuated mechanical grippers”. In: *J. Mech. Des.* 123.3 (2001), pp. 367–374.
- [16] Allison M Okamura, Niels Smaby, and Mark R Cutkosky. “An overview of dexterous manipulation”. In: *Proceedings 2000 ICRA. Millennium Conference. IEEE International Conference on Robotics and Automation. Symposia Proceedings (Cat. No. 00CH37065)*. Vol. 1. IEEE, 2000, pp. 255–262.
- [17] Jérôme Perret, Quentin Parent, and Bernard Giudicelli. “HGlove: A wearable force-feedback device for the hand”. In: *14th annual EuroVR conference*. 2017.
- [18] Matteo Rossi et al. “HapPro: a wearable haptic device for proprioceptive feedback”. In: *IEEE Transactions on Biomedical Engineering* 66.1 (2018), pp. 138–149.
- [19] Gionata Salvietti et al. “Object-based bilateral telemanipulation between dissimilar kinematic structures”. In: *2013 IEEE/RSJ International Conference on Intelligent Robots and Systems*. IEEE, 2013, pp. 5451–5456.
- [20] Marco Santello, Martha Flanders, and John F Soechting. “Postural hand synergies for tool use”. In: *Journal of Neuroscience* 18.23 (1998), pp. 10105–10115.
- [21] Gerwin Smit et al. “Efficiency of voluntary opening hand and hook prosthetic devices: 24 years of development”. In: *J Rehabil Res Dev* 49.4 (2012), pp. 523–34.
- [22] Panagiotis Sotiropoulos et al. “A benchmarking framework for systematic evaluation of compliant under-

- actuated soft end effectors in an industrial context”. In: *2018 IEEE-RAS 18th International Conference on Humanoid Robots (Humanoids)*. IEEE. 2018, pp. 280–283.
- [23] Bernhard Weber and Clara Eichberger. “The benefits of haptic feedback in telesurgery and other teleoperation systems: a meta-analysis”. In: *International Conference on Universal Access in Human-Computer Interaction*. Springer. 2015, pp. 394–405.

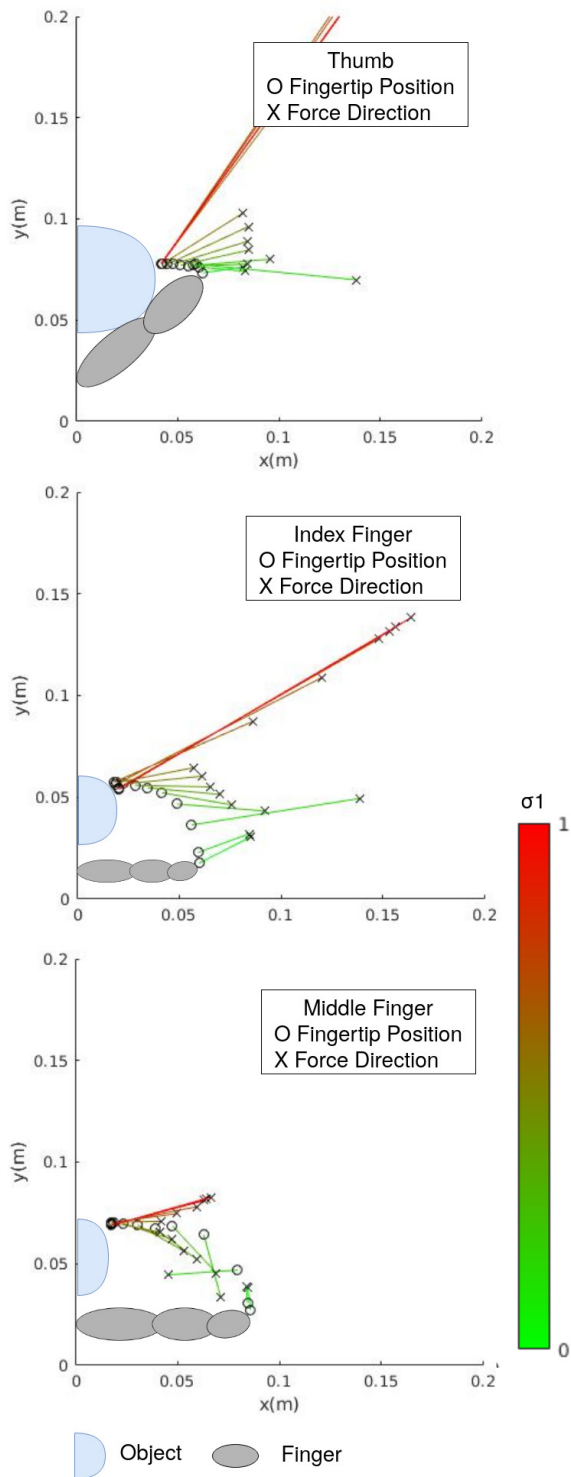


Fig. 8. Force Feedback applied on fingertips during grasping an object; Top-bottom: Thumb, Index, Middle; Colour determined by closure of the hand (0-green, 1-red)

APPENDIX A
POSITION MAPPING IN SYNERGY SPACE

This section is dedicated towards describing the mapping between cartesian space and synergy space called synergy matrix mentioned in section II-A1.

A. Creation of Synergy Mapping

In order to create a synergy mapping, a data collection experiment like the one in [6] was undertaken using the master device in section I-D to analyse the reduced dimensional synergy space. The fingertip motion data was recorded when a right-handed operator was instructed to shape the right hand as if to grasp a list of objects. The 57 objects in the list [20] included objects of a range of shapes and sizes belonging to daily sphere of life in order to capture the modulation of the hand postures during natural grasping. The data was recorded at a sample rate of 1 kHz while the operator continuously performed grasping-ungrasping motions 5 times for each of the 57 objects. The recorded data was stored in a matrix $x_{collection} \in \mathbb{R}^{n_c \times 3n}$ where n_c is the number of samples of the data collection and $3n$ is the dimension of data in each sample which is composed of $n = 3$, the number of fingers of the exoskeleton and 3 is the dimension of the space used to describe each fingertip trajectory, in this case, the cartesian position.

A PCA analysis of the collected data was carried out to verify that the collected data was strongly correlated with each other and to observe the proportion of variance of data along the principal components. Applying the PCA involves applying eigenvalue decomposition to the mean-centered data to obtain eigenvalues which represent the importance of each principal component and a matrix containing eigenvectors as columns. The eigenvectors in the matrix must be arranged according to their corresponding eigenvalues sorted from largest to smallest. The resulting matrix is called the Synergy Matrix S_x which is used as a power-continuous mapping between cartesian space and synergy space.

Similar to the results of [6], in this study the first two principal components account for more than 90% of the variance of the data, showing a stronger correlation than the PCA results of joint data in [20] in which the same parameter is 80%. This high correlation in the variables of the fingertip cartesian space permits the creation of a low-dimensional variable set constructed as a linear combination of the variables in the initial space to describe the hand posture during grasping motions.

Since the Synergy map made using PCA is independent of the reference coordinate system, there is no need to transform the fingertip data of all three fingers in a single coordinate frame as is done in other grasp estimation methods [19]. Each finger of the HGlove is a serial manipulator and therefore has its own base reference frame. The kinematics of the exoskeleton fingers f_k may be calculated in their base reference coordinate frames rather than being transformed into a single reference coordinate frame. In case a device-independent Synergy Matrix is required to be implemented, the data must be transformed to a single common reference coordinate frame.

B. Normalization of PC1 coordinate

The SoftHand accepts position commands in the range $[0, 1]$ where 0 indicates fully open hand-pose and 1 indicates fully closed hand-pose. The coordinate along PC1 for open hand-pose and closed hand-pose may differ from person-to-person and therefore, a simplified calibration procedure is proposed in [5]. In this simplified calibration procedure, the operator must move his/her hand using the exoskeleton along the first synergy, i.e. in a hand closing-opening motion such that the coordinate along PC1 is recorded for the open and closed hand-pose for every new operator. In regular operation, the PC1 coordinate is scaled to vary in the defined range and the resulting normalized PC1 coordinate is used to send position commands to the SoftHand. The entire procedure of recording fingertip cartesian position data of an operator described in the previous section need not be carried out for every new operator as experimentally validated in [5].

C. Experimental Validation

The position mapping in synergy space is validated using two experiments mentioned in section III-C of [6]. The first experiment involves motion of the operator's hand along first synergy, i.e. hand closure to grasp a random object leading to corresponding change in the position along first synergy, σ_1 as can be seen in figure 2. In the second experiment, abduction-adduction of the hand, that is, motion of the fingers in the plane of the palm itself was carried out to verify that the position along first synergy, σ_1 did not vary significantly. Therefore, it was verified that the coordinate along first synergy, σ_1 , represented hand-closure motion only which is deemed fit to be sent as position commands to the SoftHand.

APPENDIX B
INTERACTION TORQUE OBSERVER

An Interaction Torque Observer, as described in [1] and mentioned in section II-B, is necessary to be implemented in order to obtain interaction torque from the motor current of the SoftHand.

A. Structure

A robust observation technique is used to estimate the hand model torque τ_{model} and also to finally estimate the interaction torque τ_{int} . The disturbance model of the hand is created using assumptions based on the design of the SoftHand as shown in equation 10. The parameters such as frictional coefficients n_s, D and hand tendon stiffness K_{te} of the SoftHand in use were estimated by means of conventional least squares identification algorithm applied to angular displacement q and velocity \dot{q} of the motor.

$$\tau_{model} = \begin{cases} (1 + n_{s1}) K_{te} (q - q_o) + D_1 \dot{q}, & \dot{q} > 0 \\ (1 - n_{s2}) K_{te} (q - q_o) + D_2 \dot{q}, & \dot{q} < 0 \end{cases} \quad (10)$$

The interaction torque observer itself is based on equation 11 where s is the Laplace operator and λ is the filter cut-off frequency. This filter cut-off frequency λ is tuned such that it is low enough to result in a robust system, while also limiting the filtering delay. I_{ref} represents motor current, K_{tn} is the motor torque constant and J_n is the motor inertia used to estimate the τ_{int} along with estimated τ_{model} denoted with cap on top to represent that these are estimated values.

$$\hat{\tau}_{int} = \frac{\lambda}{s + \lambda} (K_{tn} I_{ref} + \lambda J_n \dot{q} - \hat{\tau}_{model}) - \lambda J_n \dot{q} \quad (11)$$

The estimated interaction torque $\hat{\tau}_{int}$ is expected to reflect the forces exerted by the environment on the SoftHand upto an extent where the stiffness of the object can also be distinctly identified. The implementation of the observer primarily involved finding a function for implementing a low-pass filter in a discrete system since C++ was the programming language used. The two candidate filters for implementing the low-pass filter were

- 1) the infinite-impulse response (IIR) filter implemented using an exponentially-weighted average function.
- 2) the finite-impulse response (FIR) filter implemented using a moving average function.

The FIR is inherently stable since the output is a finite number of finite multiples of inputs. Therefore, FIR filter implemented using a moving average function of window size 100 was chosen to be implemented in the tele-manipulation system. The filter cut-off frequency was set as 1 since it presented a good trade-off between robustness and delay. This design choice was verified by matching its output from that of a system implemented in SIMULINK using continuous system solvers.

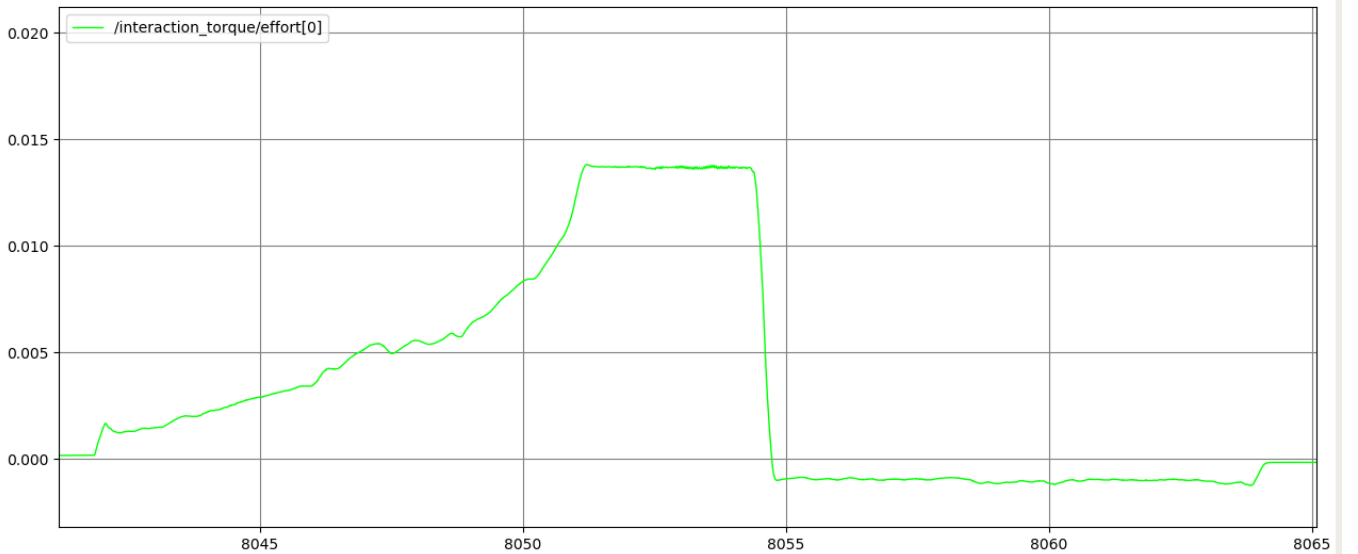


Fig. 9. Model Torque Profile of C++ implementation using ROS; Torque(N.m) v/s Time(s)

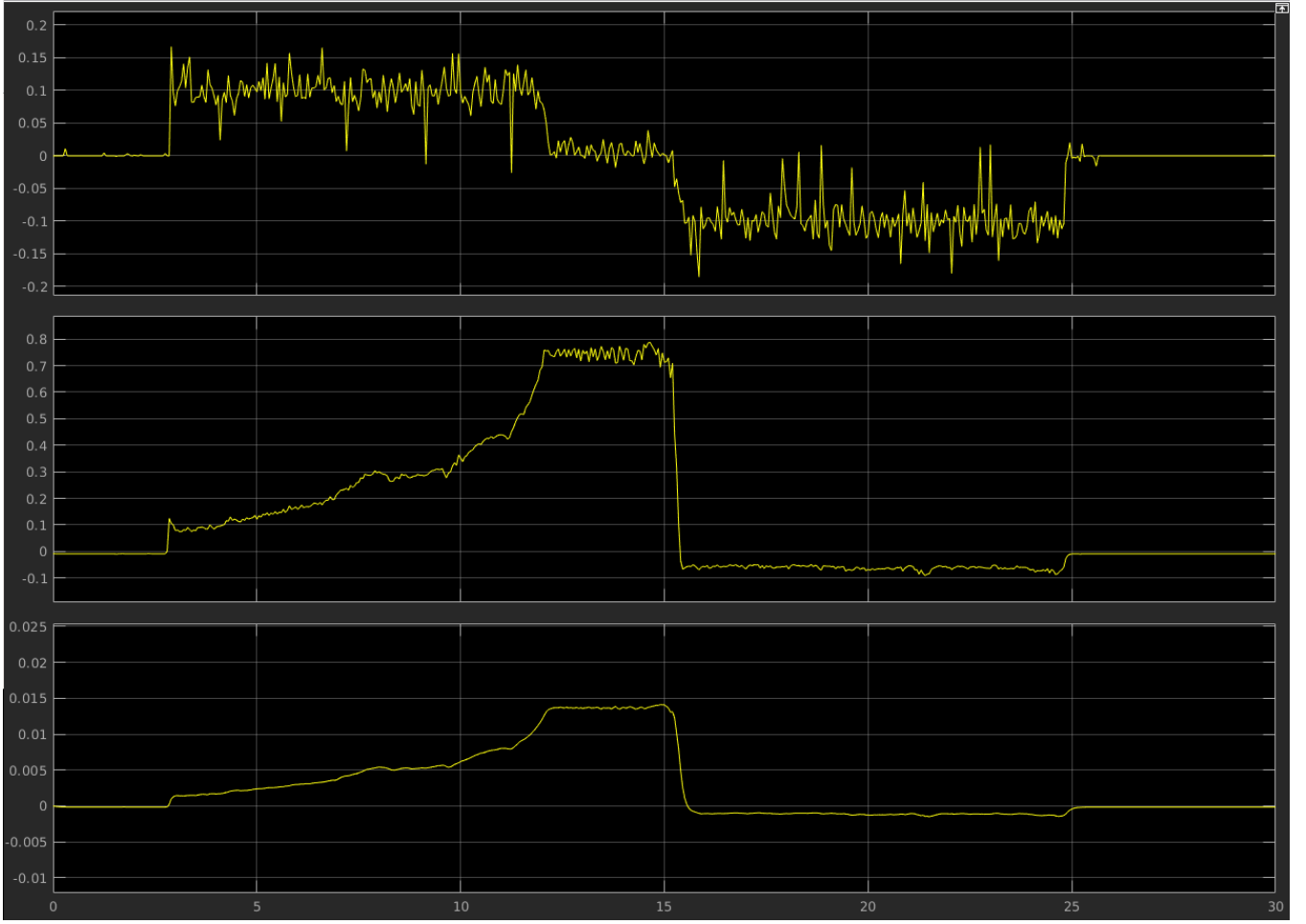


Fig. 10. Model Torque Profile of SIMULINK implementation; Top-Bottom: $\dot{\sigma}$ (/s), I_{ref} (A) and Torque(N.m) v/s Time(s)

B. Identification of Parameters of Hand Model

In order to identify the parameters of the hand model in equation 10, the hand controller was driven with fixed and low velocity trajectories (hand-closure 10% per second) from the fully open to fully closed hand-pose and in the reverse direction as explained in [1]. The model torque estimated using 13 was recorded along with the velocity and position profiles to obtain data for least squares identification algorithm. The data in the form of position and velocity profiles was represented in a $N \times 2$ regression matrix Φ_N where N is the number of data points. The corresponding model torque profile was represented in an output vector Y_N . Applying the Least-Squares Estimate (LSE) using the Moore-Penrose pseudoinverse as shown in equation 12 provided the best fit $\hat{\theta}_N$ as stated in table I

$$\hat{\theta}_N = \Phi_N^+ Y_N \quad (12)$$

The identified parameters included a position dependent coefficient $K(\sigma)$ and a velocity dependent coefficient $K(\dot{\sigma})$ each for

TABLE I
ESTIMATED PARAMETERS OF HAND MODEL

Condition	$K(\sigma)$	$K(\dot{\sigma})$
$\dot{\sigma} > 0$	8.3×10^{-3}	7.2×10^{-3}
$\dot{\sigma} < 0$	-0.2×10^{-3}	8.2×10^{-3}

the closing ($\dot{q} > 0$) and opening ($\dot{q} < 0$) motion. These coefficients were left to be functions of σ , i.e. normalized position coordinate rather than those of q , i.e. motor angular position since the position and velocity profiles were recorded as normalized coordinates.

$$\hat{\tau}_{model} = \frac{\lambda}{s + \lambda} (K_{tn} I_{ref} + \lambda J_n \dot{q}) - \lambda J_n \dot{q} \quad (13)$$

APPENDIX C
EXPERIMENTAL RESULTS OF EXISTING IMPLEMENTATION

Experiments involving grasping an object using the SoftHand controlled by the HGlove with force feedback generated as per the existing framework described in [6] were carried out as referred to in section II-B1. As can be seen in figure 11, the feedback forces are approximately directed directly towards the open hand position of the fingertips. These directions of the fingertip forces are fixed based on the synergy matrix and do not vary with the configuration or posture of the hand. Therefore while grasping smaller objects at a hand closure of about 50% or more, the forces are tangential to the surface of the object or normal to the direction of hand closure. In this case, the feedback forces guide the fingers to curl up inwards and therefore these forces cannot be said to oppose hand closure. In the experimental setup of the referred study, the exoskeleton device only had one active joint for each finger which cannot provide a good resolution of forces in the $X - Y$ plane, that is, the plane of the fingers' closing motion. This may point to the reason why the described shortcoming was not observed in the previous work.

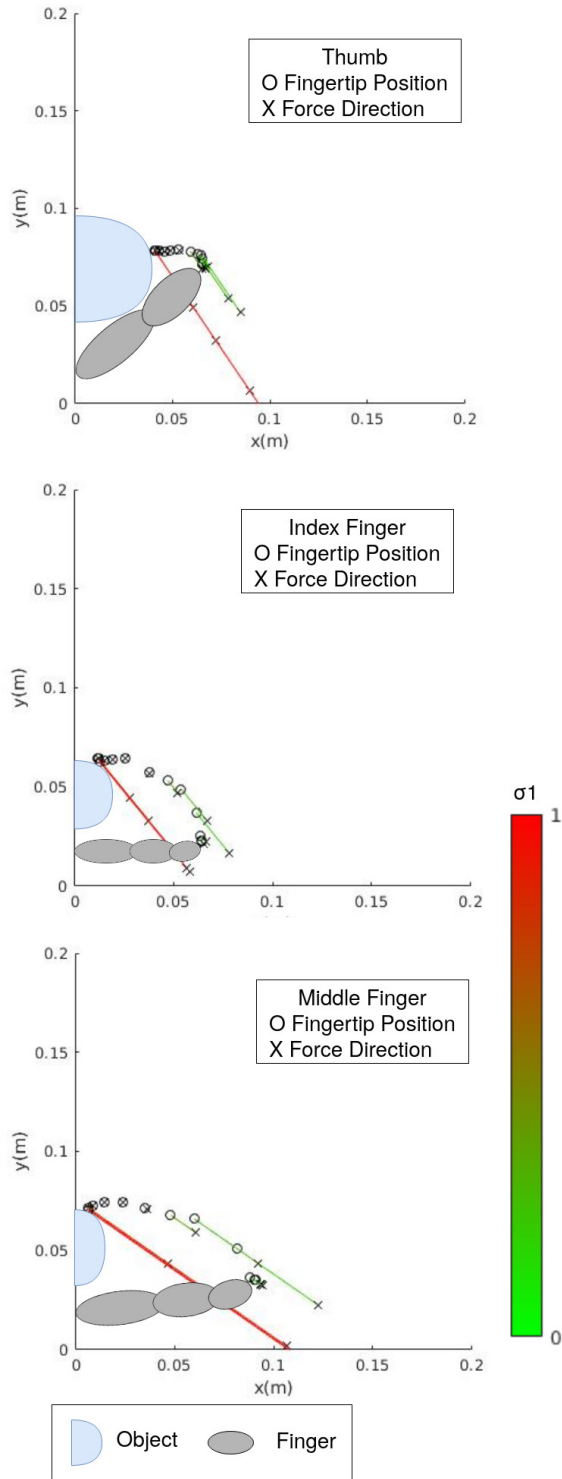


Fig. 11. Force Feedback applied on fingertips during grasping an object; Top-bottom: Thumb, Index, Middle; Colour determined by closure of the hand (0-green, 1-red)

APPENDIX D
LINEAR ESTIMATION OF SETPOINT σ

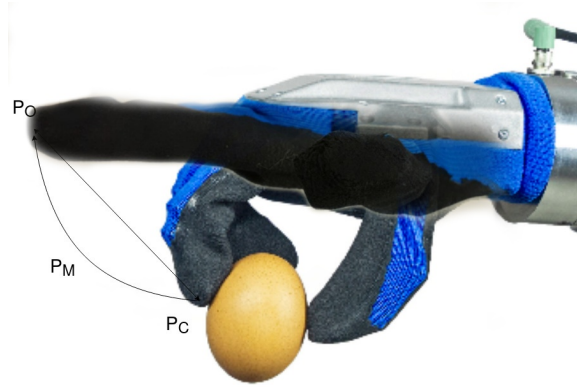


Fig. 12. Trajectory of σ linear approximation v/s database P_O - Open Hand-Pose, P_C - Closed Hand-Pose, P_M - Middle Hand-Pose

In order to generate force feedback references in section II-B2, the slave position in synergy space σ_s is estimated using a database rather than a linear estimation. This section discusses the motivation behind this design decision. It states the drawbacks of estimating the setpoint σ_s using linear interpolation between the open and closed hand-pose coordinates in the way the normalization of PC1 coordinate is done. This interpolation assumes that the position σ varies linearly during hand closure along PC1 as opposed to the complex profiles in figure 2. This approximation neglects the significant deviation in trajectory of σ_3 from a linear one. The trajectory of PC1 hand-pose setpoints estimated using this linear approximation are along a straight line as shown in 12 compared to those estimated using the PC1 hand-pose database which are along the curved line. The linear approximation, therefore, generates force feedback directly pointing towards the open hand-pose P_O which interferes with the hand-pose tracking impedance controller because the PC1 hand closure trajectory passes via point P_M rather than along the straight line. The operator's fingers are guided along the straight line trajectory rather than the PC1 hand closure which causes erroneous force-feedback for the operator during unconstrained hand closure. The difference between the two trajectories highlights the need to incorporate the complex non-linear trajectory of σ which is accomplished using the PC1 hand-pose database proposed in section II-B2.

APPENDIX E
IMPLEMENTATION DETAILS

This appendix provides details on the implementation of the system. It provides more details compared to the Method section of the paper.

A. System Overview

In this subsection, an overview of the implemented system is presented. The interconnection between the hardware and software components can be seen in figure 13. The 3 main ROS nodes `qb_hand`, `synergy_port` and `hglove` are connected using the topics that they subscribe and publish to. How to install, calibrate and run the setup is explained in Appendix F. The tele-manipulation setup is implemented in ROS using the C++ programming language.

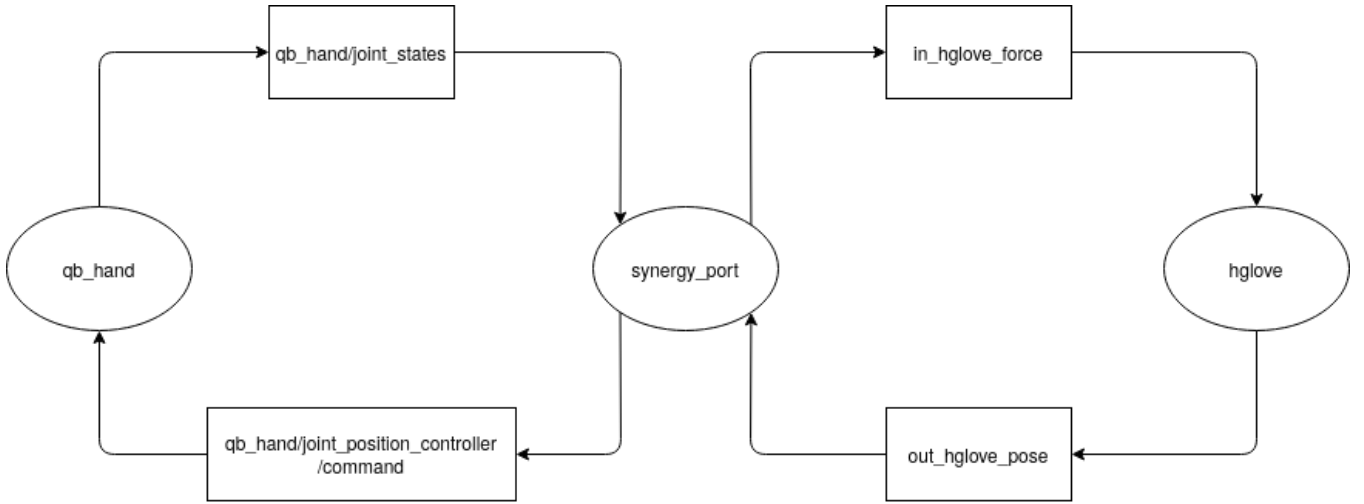


Fig. 13. Overview of the ROS Network

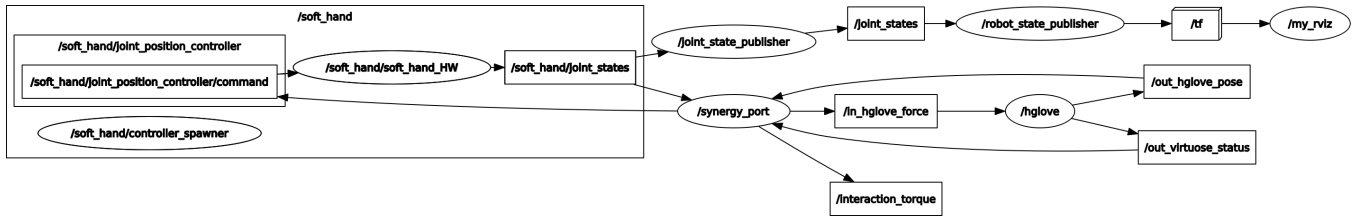


Fig. 14. Detailed ROS Network

B. QB SoftHand

The QB SoftHand was controlled using a ROS node acting as a hardware interface for the robotic hand. The `qbhand-ros` package provides this node in a configuration where the controller used is a `position_controllers/JointTrajectoryController` from the standard `ros_controllers` package. For real-time applications like tele-operation, the controller type was changed to `position_controllers/JointPositionController` to propagate the position commands to the robotic hand's local position control loop applied using effort (current) commands. The QB SoftHand also uses the `joint_state_controller/JointStateController` to present data regarding the position, velocity and current of the QB SoftHand's motor.

C. Haption HGlove

The HGlove was interfaced with the tele-manipulation system using a ROS node working along with the daemon provided by Haption. The ROS node for the HGlove was developed based on the ROS node for Virtuose by considering the data for the 3 fingers as an array stacked together starting with the thumb, index and middle finger. The ROS node for the HGlove additionally calculates the kinematics of the fingers since the data accessible from the HGlove is only in the form of joint data. A ROS package called `virtuose` is appended with the `hglove_node` as the interfacing node in addition to a `hglove_viz` as the



Fig. 15. QB SoftHand

ROS node for visualizing the HGlove's fingers as well as the forces being applied on the fingertips using RVIZ. A URDF model for the HGlove was also built only using the dimensions of the device measured physically. The kinematics of the HGlove's fingers were calculated using the `GeometricalJacobian` library present in the RAM git. Since the index and middle finger were identical, only 2 initialization functions were added to the library called `hglove_finger` and `hglove_thumb`. These functions contain the positional offsets based on the geometry of the robot to create the kinematic model of the robot.



Fig. 16. Haption HGlove

D. Synergy Port

A new ROS package called `synergy_port` was developed to implement the tele-manipulation control system presented in this work. This package contains 3 ROS nodes,

- 1) `synergy_calibration` for creation of the synergy mapping which is a one-time activity
- 2) `simplified_calibration` for calibrating the synergy mapping for every new user
- 3) `synergy_port_node` for running the tele-manipulation system

The functions performed by these nodes are stated in table II.

TABLE II
TASK PERFORMED BY THE SYNERGY PORT

Task Performed	<code>synergy_calibration</code>	<code>simplified_calibration</code>	<code>synergy_port_node</code>
Make secure connection with the haptic device	×	×	×
Read fingertip position data in cartesian space	×	×	×
Map fingertip position data to synergy space	-	×	×
Record PC1 hand-closure limits and setpoint database	-	×	-
Send position commands to SoftHand	-	-	×
Read data from SoftHand	-	-	×
Estimate interaction torque	-	-	×
Calculate force feedback in cartesian space	-	-	×
Send force feedback to the haptic device	-	-	×

APPENDIX F
INSTALLATION CALIBRATION GUIDE

This appendix provides the installation specifications for the implementation presented in the Method section of the paper and the calibration procedure prescribed for different users to use HGlove - the hand exoskeleton.

A. Installation Guide

Procedure for installing the telemanipulation setup

- Make sure Ubuntu 18.04 is installed
- Install ROS Melodic: <http://wiki.ros.org/melodic/Installation/Ubuntu>
- Install the Haptic Daemon for HGlove by following its Documentation for Linux
- Once connected, calibrate the HGlove and start the Haptic Daemon as mentioned in the Documentation (Append -- `nofork` to see the status of the daemon when running)
- Install the ROS package `virtuose` for using the HGlove
- Install the C++ library `GeometricalJacobian` from the RAM git which is required for the HGlove kinematics
- Install the ROS package `synergy_port` for using the telemanipulation controller
- Follow the documentation of QB SoftHand to connect it.
- Install the ROS package `qbhand-ros` and all its dependencies from <https://bitbucket.org/qbrobotics/qbhand-ros/src/production-melodic/>

B. Calibration Procedure

This appendix provides the detailed procedure to calibrate the synergy mapping for a particular user using nodes from the `synergy_port` package.

- 1) Ensure availability of Synergy Matrix as a file with name "Synergy_data_`_j`ANY_username`_i`.txt"
- 2) If unavailable, create Synergy Matrix by first running `synergy_calibration` node giving "HGlove_data_`_j`username`_i`.txt" as output.
- 3) Run the C++ executable `SynergyMatrix.cpp` to create Synergy Matrix of a particular user
- 4) Once Synergy Matrix is available, run `simplified_calibration` node to record "PC1_limits_`_j`username`_i`" and "setpoint_database_`_j`username`_i`" for every new user

The simplified calibration is required to be run for every new user regardless of the availability of the synergy matrix specific to that particular user. The synergy matrix need not be generated for every new user, it can be used for various users.

C. Running Procedure

Procedure for executing the telemanipulation controller setup

- 1) Once connected, calibrate the HGlove and start the Haptic Daemon as mentioned in the Documentation (Append -- `nofork` to see the status of the daemon when running)
- 2) Run the launch file which contains `synergy_port_node` to execute the telemanipulation controller along with the SoftHand and the HGlove
- 3) Manually press the green button on the HGlove's box to start force feedback.